HHS Public Access

Author manuscript

Int J Cancer. Author manuscript; available in PMC 2016 December 01.

Published in final edited form as:

Int J Cancer. 2015 December 1; 137(11): 2618–2629. doi:10.1002/ijc.29632.

Clostridium Perfringens Enterotoxin C-terminal domain labeled to fluorescent Dyes for *in vivo* visualization of micro-metastatic chemotherapy-resistant ovarian cancer

Emiliano Cocco[1,2], **Erik M. Shapiro**[3], **Sara Gasparrini**[1], **Salvatore Lopez**[1,4], **Carlton L. Schwab**[1], **Stefania Bellone**[1], **Ileana Bortolomai**[1], **Natalia J. Sumi**[1], **Elena Bonazzoli**[1], **Roberta Nicoletti**[1], **Yang Deng**[5], **W. Mark Saltzman**[5], **Caroline J. Zeiss**[6], **Floriana Centritto**[1], **Jonathan D. Black**[1], **Dan-Arin Silasi**[1], **Elena Ratner**[1], **Masoud Azodi**[1], **Thomas J. Rutherford**[1], **Peter E. Schwartz**[1], **Sergio Pecorelli**[7], and **Alessandro D. Santin**[1,*]

[1]Department of Obstetrics, Gynecology and Reproductive Sciences, Yale School of Medicine, New Haven, CT

[2]Department of Molecular and Translational Medicine, Palazzetto Polifunzionale Via Branze, 39, 25123, Brescia, Italy

[3]Department of Radiology, Michigan State University, East Lansing, MI

[4]Division of Gynecologic Oncology, University Campus Bio-Medico of Rome, Via Alvaro del Portillo 21, 00144 Rome, Italy

[5]Department of Biomedical Engineering, Yale University, New Haven, CT

[6]Department of Comparative Medicine, Yale School of Medicine, New Haven, CT, USA

[7]Division of Gynecologic Oncology, University of Brescia, Brescia, Italy

Abstract

Identification of micro-metastatic disease at the time of surgery remains extremely challenging in ovarian cancer patients. We used fluorescence microscopy, an *in vivo* imaging system and a fluorescence stereo microscope to evaluate fluorescence distribution in claudin-3 and -4 overexpressing ovarian tumors, floating tumor clumps isolated from ascites and healthy organs. To do so, mice harboring chemotherapy-naïve and chemotherapy-resistant human ovarian cancer xenografts or patient-derived xenografts (PDX) were treated with the carboxi-terminal binding domain of the *Clostridium Perfringens Enterotoxin* (c-CPE) conjugated to FITC (FITC-c-CPE) or the near-infrared (NIR) fluorescent tag IRDye CW800 (CW800-c-CPE) either intraperitoneal (IP) or intravenous (IV). We found tumor fluorescence to plateau at 30 minutes after IP injection of both the FITC-c-CPE and the CW800-c-CPE peptides and to be significantly higher than in healthy organs ($p<0.01$). After IV injection of CW800-c-CPE, tumor fluorescence plateaued at 6 hours while the most favorable tumor to background fluorescence ratio (TBR) was found at 48 hours in both mouse models. Importantly, fluorescent c-CPE was highly sensitive for the *in vivo* visualization of peritoneal micro-metastatic tumor implants and the identification of ovarian tumor

*Corresponding author: Alessandro D. Santin MD; Address: 333 Cedar Street, LSOG 305, PO Box 208063, New Haven, CT 06520-8063, USA, Telephone: 203-737-4450, Fax: 203-737-4339, alessandro.santin@yale.edu.

spheroids floating in malignant ascites that were otherwise not detectable by conventional visual observation. The use of the fluorescent c-CPE peptide may represent a novel and effective optical approach at the time of primary debulking surgery for the real-time detection of micro-metastatic ovarian disease overexpressing the claudin-3 and -4 receptors or the identification of residual disease at the time of interval debulking surgery after neoadjuvant chemotherapy treatment.

Keywords

ovarian cancer; *Clostridium Perfringens Enterotoxin*; IRDye CW800; real-time imaging; residual disease

Introduction

Ovarian cancer remains the most lethal gynecologic malignancy with 14,270 estimated deaths in the US in 2014 [1]. Due to the lack of an effective screening program, two-thirds of patients are diagnosed with late stage (III–IV) cancer with omentum, bowel, or mesentery involvement and in extreme cases, diffuse carcinomatosis [2]. Although the majority of ovarian cancer patients initially respond to the standard combination of surgery and chemotherapy, nearly 90% later develop chemotherapy-resistant tumors and inevitably succumb to their disease [3].

One of the most important prognostic factors for patients with ovarian cancer is the size of residual disease after surgical cytoreduction. Consistent with this, in multiple studies the subset of patients achieving optimal cytoreduction (≤1cm residuum) after primary debulking surgery or after neoadjuvant chemotherapy followed by interval debulking surgery have superior outcomes when compared to patients left with macroscopic amounts of residual disease [3]. Thus, improving our ability to resect tumors via highly sensitive, real-time, intra-operative detection systems to visualize microscopic metastatic disease would likely yield better patient outcomes. Accordingly, the first in-human intraoperative tumor-specific fluorescence imaging in ovarian cancer has recently been reported [4]. In this study folate conjugated to fluorescein isothiocyanate (folate-FITC) was used to guide surgeons to identify small-size tumor deposits in the abdominal cavity of patients with folate receptor α (FRα) overexpressing ovarian cancers. In this pilot study, surgeons were able to identify a significantly higher number of tumors when assisted by the tumor-specific fluorescent system when compared to using conventional visualization alone [4]. FRα expression has been reported in the majority of epithelial ovarian cancer [5, 6]. Importantly, recent studies also showed that its expression is retained after chemotherapy, identifying FRα as a potential target for chemotherapy-resistant disease [78].

Our research group has analyzed the genetic fingerprints of a large number of epithelial ovarian cancers [9–12]. In these studies we discovered Claudin-3 and Claudin-4 as two of the top differentially expressed genes in all histological ovarian cancer types tested [9–12]. Furthermore, additional studies by our group and others have shown chemotherapy-resistant and recurrent ovarian cancers to express significantly higher levels of Claudin-3/4 compared to matched chemotherapy-naïve tumors [13, 14]. We also found overexpression of Claudin-4 in the chemotherapy resistant subpopulation of CD44-positive ovarian cancer cells [15]. Taken

together, these data suggest that Claudin-3/4 may represent ideal molecular targets for the detection/treatment of chemotherapy-resistant/recurrent ovarian cancers.

Claudin-3/4 are the natural epithelial receptors for *Clostridium Perfringens Enterotoxin* (CPE), a single polypeptide of 319 amino acids that is associated with *C. Perfringens type A* food poisoning [16]. The interaction of CPE with Claudin-3/4 results in membrane permeability changes, osmotic cell ballooning and finally cell death [16–18]. Remarkably, although the systemic administration of the full length CPE in mice is toxic, limiting its use to local therapies, the injection of the carboxy-terminal fragment (i.e., the c-terminal 30aa, c-CPE) is devoid of any toxicity while preserving the binding affinity to the receptors [16]. Therefore, the use of c-CPE as a carrier for diagnostic/real-time imaging contrast agents or for therapeutics can represent a novel approach for the potential detection/treatment of Claudin-3/4 overexpressing ovarian tumors [19].

Accordingly, we have recently reported that FITC conjugated c-CPE peptide (FITC-c-CPE) specifically binds and internalizes into Claudin-3/4 overexpressing ovarian cancer cells *in vitro*. Our previous results also showed that FITC-c-CPE localizes to chemotherapy-resistant tumors *in vivo* in xenograft mouse models following intravenous (IV) FITC-c-CPE administration [20]. Unfortunately, although FITC-c-CPE showed high tumor-targeting specificity in *ex vivo* models, its potential use in the intraoperative setting for the optical detection of residual disease in real-time was not possible secondary to the major limitations in the use of the FITC-fluorescence *in vivo* [i.e., the high absorption and scattering that occur in biological tissues in the visible light spectrum between 390 and 700nm, range that includes the excitation and emission wavelengths of the FITC molecule (480/535nm, respectively)]. Importantly, recent studies have demonstrated that Near-InfraRed (NIR) fluorescent Dyes (excitation >750nm) are the preferred in vivo fluorophores for labeling targeted ligands due to their deep tissue penetration and the lack of organs autofluorescence at such wavelengths [21].

In this study, we have a) extended our previous research evaluating the *in vivo* kinetics and biodistribution of FITC-c-CPE following intraperitoneal (IP) administration of the labeled peptide into mice harboring metastatic and chemotherapy-resistant ovarian cancer, b) conjugated c-CPE to the IRDye CW800 to generate CW800-c-CPE and carefully evaluated the kinetics and tumor binding capacity of this peptide *in vivo* following IP or IV injection in xenograft models of chemotherapy-resistant ovarian cancer and PDXs and c) evaluated the ability of CW800-c-CPE to identify micro-metastatic sites of disease in the abdominal cavity of SCID mice harboring highly relevant xenograft models of chemotherapy-naive and chemotherapy-resistant human ovarian cancer using a fluorescence stereo microscope.

Materials and Methods

Peptides synthesis

The FITC conjugated *Clostridium Perfringens* carboxy-terminal fragment CPE peptide (FITC-c-CPE) was synthesized by InVitrogen (Grand Island, N.Y.), with the sequence (FITC)-SLDAGQYVLVMKANSSYSGNYPYSILFQKF and a purity level >95%. IRDye CW800 maleimide was purchased from LI-COR (Lincoln, NE). Briefly, 0.5 mgs of Dye

were resuspended in DMSO and used for the conjugation of the IRDye to a modified version of c-CPE (we introduced a Cysteine at N-terminal of c-CPE sequence in order to promote the reaction between the thiol group of the Cysteine and the maleimide group attached to the IRDye CW800) that was synthesized and purified by Keck Biotechnology Resource Laboratory (Yale University) with a purity level of >95%. Conjugation was performed in the dark in the presence of excess IRDye. After 2 hours of incubation at Room Temperature (RT), the conjugate was dialyzed against water. Conjugation was verified by Matrix-assisted laser desorption/ionization (*MALDI*) analysis and concentration of CW800-c-CPE evaluated by Bio-Rad Assay (Hercules, CA).

SCID xenograft mouse models

C.B-17/SCID female mice 5–7 weeks old were purchased from Harlan Sprague-Dawley (Indianapolis, IN) and housed in a pathogen-free environment at Yale University. They were given basal diet and water ad libitum. All experimental procedures were approved by the Institutional Animal Care and Use Committee. In this study, ARK-1, a chemotherapy-resistant primary ovarian serous papillary carcinoma (OSPC) cell line, was used to develop multiple xenograft models. This cell line was established from samples collected at the time of tumor recurrence from a patient harboring stage IV OSPC. This primary cell line was chosen because of its high resistance to multiple chemotherapeutic agents verified by *in vitro* Extreme Drug Resistance assay (Oncotech Inc. Irvine, CA) [22] and its extremely elevated expression of Claudin-3/4 recently evaluated by our group [20]. Briefly, the OSPC-ARK-1 cancer cell line was injected IP at a dose of 7×10^6. Six to eight weeks later, when tumor nodules were 0.5–0.8 cm in size, 10μg of FITC-c-CPE or CW800-c-CPE were injected IP. At different time points, mice were sacrificed and fluorescence of tumors and excised normal organs was visualized using an In-Vivo FX PRO system (Bruker Corporation, Billerica, MA; excitation/emission 480/535nm and 760/830nm for the visualization of FITC-c-CPE and CW800-c-CPE, respectively). Pictures of tumors and organs excised from animals not injected with the fluorescent peptides were captured using the same setting to evaluate tissue autofluorescence. Fluorescence quantification was calculated using the Molecular Imaging Software 7.1.1. Alternatively, C.B-17/SCID mice were injected subcutaneously with 5×10^6 cells derived from OSPC-ARK-1. After 4–5 weeks, 25μg of CW800-c-CPE were injected IV and whole body fluorescence imaging was performed at different time points ranging from 30 minutes to 96 hours using the In-Vivo FX PRO system. *In* vivo whole body time course experiments were also performed on patient derived xenograft (PDX) models of chemotherapy-naïve and chemotherapy-resistant ovarian cancers. Metastatic models of ovarian cancer were generated following the injection of OSPC-ARK-1 derived cells into multiple sites in the abdominal cavity of 5–7 weeks old mice. After 6–8 weeks, 10 to 25μg of CW800-c-CPE were injected IP or IV. At different time points, animals were sacrificed and the abdominal cavity was opened. Ovarian tumor as well as metastatic implants spread in the abdomen were excised and visualized using the In-Vivo FX PRO system. Additionally, 2 control tumor-bearing animals were injected IV with an equimolar concentration of unlabeled CW800 and whole body time course imaging was performed using the same excitation/emission protocol.

Fluorescence microscopy

C.B-17/SCID mice harboring xenografts of metastatic OSPC-ARK-1 chemotherapy-resistant tumor were generated by IP injection of tumor cells in multiple sites of the abdomen. After 6–8 weeks, tumor implanted mice were injected IP with 10μg of FITC-c-CPE. Mice were sacrificed 12 hours later and the abdominal cavity was opened. Real-time fluorescence imaging for the identification of metastatic implants disseminated in the abdomen was carried out with a fluorescence stereo microscope (M205FA) using an EL6000 external light source (Leica microsystem). The FITC filter cube was a 472/30nm exciter, 520/35nm emitter (acquisition time: 10 seconds). Alternatively, tumor-bearing mice were injected IV with 25μg of CW800-c-CPE. After 48 hours, animals were sacrificed and the abdominal cavity was opened. Real-time fluorescence imaging was carried out with a fluorescence stereo microscope (M205FA) installing a NUANCE EX camera (Advanced Molecular vision, UK) for the detection of NearInfraRed (NIR) light using a SPECTRA X light engine external light source (Leica microsystem). The NIR filter cube was a 710/75nm exciter, 810/90nm emitter (acquisition time: 6 seconds).

Immunofluorescence on tumor clumps isolated from ascites

C.B-17/SCID mice developing ascites were generated following IP injection of 5×10^6 OSPC-ARK-1-derived cells. When ascitic fluid was abundant in the abdomen (i.e., 10–12 weeks later), animals were injected with 10μg of FITC-c-CPE IP and 12 hours later, immunofluorescence was performed on Ficoll-Hypaque separated cells isolated from ascites. Briefly, mice were anesthetized and abdominal paracentesis was performed. Cell pellet was isolated through a Ficoll gradient and an anti-human CD326 (EpCAM) PE conjugated antibody (#12-9326-42 eBioscience, San Diego, CA) was used to label the tumor cells. Images were captured using an Axio Observer.Z1 inverted fluorescence microscope (Zeiss, Germany) installing a X-cite 120Q illuminator (Lumen Dynamics, UK) and analyzed with Volocity software (Improvision, Perkin Elmer, MA). Cells isolated from the ascites of mice not injected with FITC-c-CPE were used as a control.

Histologic staining

Paraffin-embedded section slides from the specimens analyzed in this study were cut by the Research Histology Department at Yale. Slides were stained with hematoxylin-eosin (H&E) and also used for the immunofluorescence. Briefly, slides were deparaffinized with Shandon Histosolve Xylene Substitute (Thermo Scientific) and rehydrated with alcohol of anti-concentration gradient. Antigen retrieval was accomplished by pretreatment module heating at 97°C for 30 minutes. Nonspecific binding was then blocked with 10% goat serum. Slides were washed and incubated overnight at 4°C with a mouse anti-human EPCAM antibody (#2929S, Cell signaling) 1:250 in PBS. After incubation, slides were washed and incubated 30 minutes with a secondary goat anti-mouse antibody alexa fluor 488-conjugated (A11001, Invitrogen) diluted 1:4000 in PBS. After incubation, slides were washed and stained with Hoechst 33328 for 10 minutes (1:5000 RT). Images were captured using an Axio Observer.Z1 inverted fluorescence microscope and analyzed with Volocity.

Statistical analysis

Statistical comparisons between groups were done by the unpaired Student's t test using Microsoft Excel. $P<0.05$ was considered statistically significant.

Results

In vivo distribution of FITC-c-CPE following IP injection in mice harboring chemotherapy-resistant ovarian cancer

To determine whether FITC-c-CPE is able to localize to chemotherapy-resistant ovarian tumor cells *in vivo* after IP administration, SCID mice harboring OSPC-ARK-1-derived tumor xenografts were injected IP with FITC-c-CPE (10μg). At different time points, ranging from 30 minutes to 24 hours after c-CPE injection, tumors were excised and visualized using an *in vivo* FX PRO system. Fluorescence plateaued 30 minutes after IP injection of FITC-c-CPE. Mean Fluorescence Intensity (MFI) of the tumors calculated for each time point was significantly higher compared to MFI of tumors excised from non-injected control mice (MFI ±STDV = 382.4 ±54.2 for control tumors vs 768.2 ±207.4 for experimental tumors 30 minutes after c-CPE injection, $p=0.029$; 741.7 ±124.2 for tumors 6 hours after c-CPE injection, $p=0.02$; 719.4 ±190.2 for tumors 12 hours after c-CPE injection, $p=0.03$; and 584.4 ±61.8 for tumors 24 hours after c-CPE injection, $p=0.01$; Figure 1A–B). To evaluate the distribution of the FITC-c-CPE in tumor bearing animals, MFI was calculated over the ovarian tumors as well as multiple explanted organs including kidney, liver, spleen, lungs and heart at 30 minutes after IP injection of FITC-c-CPE. MFI of the tumors were found to be significantly higher than MFI calculated for each of the normal organs (Figure 1C; $p<0.01$).

Identification of metastatic ovarian cancer cells *in vivo* using FITC-c-CPE

To test the ability of FITC-c-CPE to detect small-size tumor nodules *in vivo*, metastatic tumors of the OSPC-ARK-1 primary chemotherapy-resistant ovarian cancer cell line were induced following inoculation of cancer cells in multiple sites within the animal abdomen. After six to eight weeks, mice were injected IP with 10μg of FITC-c-CPE. After incubation, the peritoneal cavity was opened and visualized using a fluorescence stereo microscope (filters setting: excitation 472/30nm, emission 520/35nm). As representatively shown in Figure 2A, metastatic implants, only a few millimeters in diameter, fluoresced intensely compared to the normal tissues in the abdomen (Figure 2A). Importantly, when mice were injected with FITC-c-CPE, strong fluorescence was detected on malignant tumor spheroids isolated from the ascitic fluid while no fluorescence was visible on tumor associated inflammatory cells (Figure 2B). These data suggest that fluorescent c-CPE may have the potential to target early occult metastatic or recurrent disease by detecting clumps of tumor cells that are not clinically visible *in vivo*.

Generation of CW800-c-CPE and *in vivo* distribution

CW800-c-CPE was generated by conjugating the IRDye CW800 to a modified version of the c-CPE (See Materials and Methods). To test whether the conjugation of CW800 to c-CPE could alter peptide binding affinity to Claudin-3/4, OSPC-ARK-1 cells were incubated

with CW800-c-CPE or FITC-c-CPE in the presence of an equimolar concentration of the full length CPE toxin. The viability of the cells was evaluated 2 hours later. Tumor cells were protected from the cytotoxic effect of CPE at a similar extent by both peptides, suggesting that the conjugation of the IRDye to c-CPE doesn't affect peptide binding properties (Supplementary Figure S1). To further evaluate the distribution of CW800-c-CPE in tumors and normal organs, mice harboring intraperitoneal human ovarian cancer were injected IP with 10μg of CW800-c-CPE and euthanized at different time points ranging from 30 minutes to 24 hours. Tumors as well as normal organs were excised and fluorescence was visualized using an In-Vivo FX PRO system (excitation 760nm, emission 830nm). MFI of tumors peaked 30 minutes after IP injection of CW800-c-CPE and was significantly higher compared to MFI calculated for the other normal organs considered (MFI, mean ±STDV: 156.55 ±23.73 in the tumor, 95.72 ±18.19 in the kidney, 30.68 ±5.88 in the liver, 23.33 ±4.05 in the spleen, 34.71 ±12.71 in the bowel, 28.16 ±6.14 in the lungs, 13.46 ±1.35 in the brain and 19.78 ±5.43 in the heart; $p<0.01$; Supplementary Figure S2). In light of these results, further *in vivo* experiments were carried out 30 minutes after IP injection of CW800-c-CPE.

Identification of metastatic chemotherapy-resistant ovarian cancer cells *in vivo* following IP injection of CW800-c-CPE

The ability of CW800-c-CPE to identify metastatic chemotherapy-resistant ovarian cancer cells was tested after IP injection of CW800-c-CPE in mice harboring intraperitoneal metastatic OSPC-ARK-1-derived tumors. As representatively shown in Figure 3A, strong fluorescence was detected on metastatic lesions of few millimeters attached on the liver and other abdominal organs of tumor bearing mice while negligible signal was observed in the surrounding healthy tissue (Figure 3A). Immunofluorescence using an anti-human EPCAM antibody was performed to confirm the histology of all the metastatic implants identified by CW800-c-CPE. As demonstrated in Figure 3B, the highly fluorescent tumor implants identified in the abdominal cavity were confirmed to represent metastatic OSPC-ARK-1 tumor cells by the anti-human EPCAM antibody.

In vivo tumor targeting capacity of CW800-c-CPE following systemic (IV) injection

Although the peritoneal cavity is the main site of disease in ovarian cancer patients and the IP route of administration is easily accessible for injection of dyes or chemotherapy agents in mice and humans, IV injection of therapeutics and contrast agents still represents the most common route of administration in the management of ovarian cancer [23]. The biodistribution of CW800-c-CPE was therefore tested *in vivo* after IV administration of 25μg of the fluorescent peptide to mice harboring subcutaneous human chemotherapy-resistant ovarian cancer. At different time points after c-CPE injection (ranging from 6 to 96 hours) mice were anesthetized and whole body fluorescence distribution was visualized using an In-Vivo FX PRO system. As shown in Figure 4, at an early time point CW800-c-CPE rapidly distributed in the tumor as well as all well-perfused normal organs while longer incubation times (24–96 hours) resulted in selective c-CPE accumulation into the tumor (Figure 4A). To determine the best incubation time for the identification of the tumor margins, MFI was calculated at the different time points in the subcutaneous tumors as well as in the surrounding adjacent tissue considered as background fluorescence. Tumor-to-

background ratio (TBR) peaked 48 hours after IV injection of CW800-c-CPE (Figure 4C). Remarkably, similar distribution was obtained after IV injection of CW800-c-CPE in patient derived xenograft (PDX) models generated from chemotherapy-naïve as well as chemotherapy-resistant ovarian cancer patients (Figure 4B–C). Interestingly, our kinetic studies are consistent with the recent data obtained by another research group that also identified the most favorable TBR time point to be 48 hours after injection of RGD conjugated to the IRDye CW800 in mouse models of glioblastoma [24]. On the basis of these results, this incubation time was chosen for further studies. Importantly, in control experiments, CW800-c-CPE targeting specificity was verified after IV injection of equimolar concentration of unlabeled CW800 dye into mice with sized-match OSPC-ARK-1-derived subcutaneous tumors. After injection with free dye, negligible labeling was detected in the tumor at the different time points tested (ranging from 24 to 72 hours; data not shown), indicating that the binding of c-CPE to Claudin-3/4 is essential to confer tumor specificity to the imaging system. Importantly, mice injected IV and/or IP with CW800-c-CPE peptide at doses ranging from 10 to 100 μg and kept under observation for up to 3 months did not demonstrate any evidence of acute or chronic toxicity (i.e., weight loss, alopecia or behavioral changes) or organotoxicity at the time of necropsy (data not shown).

Identification of micro-metastatic chemotherapy-resistant ovarian cancer cells *in vivo* following IV injection of CW800-c-CPE

The potential of CW800-c-CPE to identify small-size metastatic lesions *in vivo* was tested by injecting mice harboring intraperitoneal human chemotherapy-resistant ovarian cancer with 25μg of CW800-c-CPE IV. Mice were sacrificed 48 hours later and the abdominal cavity was opened. Primary ovarian tumors as well as multiple metastatic implants were excised and fluorescence was visualized using an In-Vivo FX PRO system. As representatively shown in Figure 5, strong fluorescence was detected on the ovarian tumor as well as on a metastatic tumor deposit of few millimeters detected on the lesser curvature of the stomach of the tumor bearing mouse (Figure 5B–C). Importantly, while no fluorescence was detected on the stomach, a weak CW800-c-CPE positive staining was visible on the visceral peritoneum of the uterus. Further histological analysis found this fluorescent site to represent an area of the uterus involved by a tiny ovarian tumor implant (Figure 5C, Supplementary Figure S3). These data demonstrate that CW800-c-CPE has exquisite sensitivity for the identification of microscopic metastatic tumor deposits otherwise not detectable by conventional visual observation. Of interest, in this in vivo model of chemotherapy-resistant human ovarian cancer, cells injected IP were able to implant/metastasize directly to the ovary. These data indicate that our preclinical ovarian cancer model may accurately resemble ovarian cancer development in patients (Figure 5A–B).

In vivo identification of microscopic metastatic ovarian cancer cell deposits by real-time imaging using CW800-c-CPE

To assess the ability of CW800-c-CPE to identify micro-metastatic ovarian cancer cell deposits *in vivo*, mice harboring intraperitoneal metastatic OSPC-ARK-1-derived ovarian tumors were injected with 25μg of CW800-c-CPE IV. After 48 hours, the abdominal cavity was opened and real-time fluorescence imaging was carried out using a fluorescence stereo

microscope installing a NUANCE EX multispectral camera. As representatively shown in Figure 6, intense fluorescence signal was detected not only in large (i.e., 10–12 mm) tumor masses located in the lower left abdomen of the mouse (Figure 6A: blue arrow), but also in 1 mm areas of the intestine where disease was not detectable by conventional visual observation (Figure 6A: green arrow). To assess whether the fluorescent signal identified on the intestine corresponded to an area of tumor cells infiltration, the fluorescent specimen was resected and immunostaining and histologic analyses were performed on multiple slides (Figure 6B–C). As shown in Figure 6C, both immunofluorescence (IF pictures) and H&E staining (H&E pictures) revealed the presence of ovarian cancer cell implants adherent to the serosa of the mouse intestine, confirming the exquisite sensitivity of the CW800-c-CPE peptide to visualize in real-time microscopic ovarian tumor deposits. Importantly, the ability of CW800-c-CPE in identifying in vivo sub-millimeter/micro-metastatic tumor implants was also verified in a PDX model of chemo naïve ovarian cancer (Supplementary Figure S4) as well as in xenograft models of chemotherapy-resistant uterine serous carcinoma (USC), a highly aggressive subtype of endometrial cancer also known to overexpress Claudin-3 and -4 [25] (Supplementary Figure S5).

Discussion

Optimal tumor debulking is one of the crucial prognostic factors in ovarian cancer, suggesting that intraoperative tumor-specific image-guided surgery may represent a valid approach to better define tumor margins, improve tumor resection and ultimately lead to better patient outcome. In this study we demonstrated for the first time the use of the C-terminal binding domain of *Clostridium Perfringens Enterotoxin* (c-CPE) conjugated to NIR-fluorescent tags for real-time optical imaging of Claudin-3/4 overexpressing chemotherapy-naïve and chemotherapy-resistant human ovarian cancer *in vivo*. The capacity of the non-toxic fluorescent c-CPE to identify microscopic metastatic tumor deposits within the abdominal cavity of tumor bearing mice, together with the overexpression of Claudin-3/4 (i.e., the CPE receptors) by the majority of ovarian carcinomas, make this optical imaging system an ideal intraoperative tool for the guidance of surgeons in the detection and resection of residual malignant disease not detectable by the conventional visual observation.

In a recent study, Van Dam et al. demonstrated for the first time in humans that the use of fluorescein isothiocyanate (FITC) conjugated to folate is an effective intraoperative fluorescent imaging system for real-time visualization of tumor tissue in patients with folate receptor α (FRα) overexpressing ovarian cancer [4]. This study unambiguously identified tumor-targeted fluorescence imaging as a suitable technique to assist surgeons during cytoreductive surgery and clearly demonstrated that penetration depth of the fluorescein signal may allow the identification of superficial peritoneal metastases in the abdominal cavity of ovarian cancer patients [4–6, 8].

Claudin-3/4 were recently found by our group as well as others to be preferentially overexpressed in multiple histological types of ovarian cancer [9–12]. Interestingly, these receptors were found to be more expressed in chemotherapy-resistant ovarian cancers when compared to chemotherapy-naïve ovarian tumors as well as in the subpopulation of CD44-

positive cancer cells with stem cells properties, thought to be responsible for the development of drug resistance and tumor relapse[13, 14, 2615]. This suggests that the c-CPE-based fluorescence imaging system may be exploited for the management of patients receiving neo-adjuvant chemotherapy for the identification of residual viable disease at the time of interval debulking. In a recent report our research group showed that c-CPE conjugated to FITC (FITC-c-CPE) binds and internalizes into multiple Claudin-3/4 primary ovarian carcinomas *in vitro* and localizes to chemotherapy-resistant ovarian cancer xenografts *in vivo* following systemic (IV) administration [20]. More importantly, we also reported accumulation of FITC-c-CPE into tumor clumps isolated from mouse ascites, suggesting the potential ability of the fluorescent c-CPE to target small tumor deposits in patients harboring metastatic or recurrent disease [20].

In this study we initially investigated the kinetics and organ biodistribution of FITC-c-CPE following intraperitoneal (IP) injection. This route of administration has recently been shown to be highly effective for the delivery of chemotherapy in ovarian cancer, a disease that arises and remains confined to the abdominal cavity in the majority of patients [23]. Our study includes data from time-course experiments *in vivo* following IP FITC-c-CPE administration in animals harboring chemotherapy-resistant human ovarian cancer. The results of our experiments show detectable uptake of FITC-c-CPE by the tumor starting 30 minutes and up to 24 hours after peptide injection. Remarkably, FITC-c-CPE bound rapidly to the tumor and allowed detection of small-size tumor implants spread into the upper abdomen and accumulated into tumor spheroids isolated from mouse ascites following abdominal paracentesis or surgery. These data confirm and expand the results we obtained after IV injection of the FITC-c-CPE peptide in previous studies [20] and pinpoint the great potential of a c-CPE-based optical imaging for the identification of occult metastatic disease not localizable by conventional visual observation after IP FITC-c-CPE injection. Importantly, our results also suggest the IP route of injection of the fluorescent c-CPE as a novel approach to be considered for diagnostic/real-time imaging purposes in ovarian cancer patients.

This study also sought to characterize the binding properties of c-CPE conjugated to a new synthetic NearInfraRed Dye (CW800) [27]. Investigation into CW800 labeled c-CPE is warranted because the excitation and the emission wavelengths of the FITC molecule (480–535nm, respectively) are in a region of the spectrum where significant tissue autofluorescence exists, therefore affecting sensitivity of FITC-based fluorescence imaging systems. Emerging data identified the nearinfrared (NIR) fluorescence imaging as the preferred optical imaging technology due to the low absorption and autofluorescence of biological tissues at high wavelengths (>750nm) that results in minimal background interference and improved tissue penetration which may allow visualization of metastatic disease up to approximately 5–8 mm of depth in parenchymal organs [21, 28–30]. Consistent with this, Indocyanine green (ICG), a FDA approved NIR dye, is currently used as angiographic contrast agent for vessel visualization during surgery and more recently, as a contrast agent for the real-time visualization of sentinel lymph nodes during lymphatic mapping [31–33]. Due to the chemical structure of ICG, its conjugation with targeting molecules (i.e., tumor-specific peptides) is extremely challenging limiting its use as a single

agent or encapsulated into delivery systems (i.e., nanoparticles) [34, 35]. Conversely, CW800 has recently earned attention in cancer imaging because of its safe administration profile and the presence of reactive functional groups in its chemical structure that allow stable conjugation with targeting molecules [27]. Tanaka et al. in 2006 reported the use of CW800 conjugated to human serum albumin for the sentinel lymph node mapping and surgical resection in preclinical models of spontaneous melanomas [36]. Moreover, the simultaneous labeling of Trastuzumab with ^{111}In and CW800 was used to generate a radio-optical tracer for tracking Her2 overexpressing breast tumors in xenografted nude mice [37]. More recently, Keereweer et al. coupled CW800 to the epidermal growth factor (EGF) or to the 2-Deoxi-D-glucose (2-DG) to target oral cancer and cervical lymph node metastases *in vivo* based on their high expression of epidermal growth factor receptor (EGFR) and/or intense metabolic activity. Authors reported co-localization between the bioluminescence signal coming from tumor luciferase expressing cells and fluorescence, thus concluding that CW800 EGF and CW800 2-DG may be used for real-time image-guided surgery aimed at achieving complete surgical resection in oral cancer patients [38]. An elegant study by Terwisscha et al., recently compared the distribution and the kinetic of Bevacizumab and Trastuzumab conjugated to the IRDye 800CW or to ^{89}Zr for optical and nuclear imaging of ovarian and gastric cancer. Authors showed that both optical and nuclear imaging modalities had the capacity to visualize the tumor with a comparable kinetic. More importantly, when they tested Bevacizumab-800CW and Trastuzumab-800CW for the intraoperative visualization of ovarian and gastric cancer, they found that the conjugated antibodies were able to identify submillimiter tumor lesions hardly visible by naked eyes [39]. Interestingly, several clinical trials using Bevacizumab and Cetuximab conjugated to IRDye 800CW for the intraoperative visualization of malignant tissue are currently ongoing in rectal (NCT01972373), esophageal NCT02129933) and head and neck (NCT01987375) cancer. Results from these studies are eagerly awaited to determine the validity of this real time optical imaging system in the intraoperative setting.

In the current study we show that CW800-c-CPE and FITC-c-CPE have similar binding affinity to Claudin-3/4 *in vitro* and comparable biodistribution *in vivo*. However, the little organ autofluorescence in the NIR region of the light spectrum suggests that CW800-c-CPE may identify tumor margins with a higher sensitivity than FITC-c-CPE, which allows for better discrimination between normal and malignant tissues. In support of this hypothesis, real-time fluorescence imaging experiments in vivo showed accumulation of CW800-c-CPE in tiny areas of the mouse intestine where no visible disease was detectable by naked eyes. Importantly, CW800-c-CPE was also able to identify microscopic metastatic tumor deposits in a USC xenograft mouse model as well as in fresh ovarian PDXs derived from patients harboring chemotherapy-naïve and chemotherapy-resistant disease. These latter models are known to retain the histologic and genetic characteristics of their donor tumor and remain stable across passages. More importantly, PDX have been shown to be more predictive of clinical outcome in drug evaluation studies and are therefore preferable for preclinical biomarker identification and validation [40]. Taken together, these data suggest that our imaging system may be suitable for the management of gynecologic malignancies other than ovarian cancer and clearly demonstrate the exquisite sensitivity of CW800-c-CPE for the

detection of microscopic implants of chemotherapy-naïve and chemotherapy-resistant-metastatic disease overexpressing the claudin-3 and/or -4 receptors *in vivo*.

Importantly, several intraoperative devices for the visualization of NIR fluorescence are currently available. Among these systems the Fluorescence-assisted Resection and Exploration (FLARE™, Frangioni laboratory, Boston, MA), the Photodynamic Eye (PDE; Hamamatsu Photonics, Hamamatsu, Japan), the SPY *Elite*™ (Novadaq Technologies, Inc., Canada), the Artemis Intra-operative multispectral imaging system (O2 view, Marken, The Netherlands) and the da Vinci Fluorescence Imaging Vision System (Intuitive Surgical, Sunnyvale, CA) have already been successfully used for human clinical applications [9, 21, 41–43]. These observations, combined with the knowledge that CW800-c-CPE is non-toxic and is able to accumulate efficiently within metastatic tumor deposits in few hours, confer our optical imaging system with tremendous translational potential.

In conclusion, in this study, we describe for the first time the potential of c-CPE conjugated to fluorescent tags as a novel optical imaging system for the real-time intraoperative visualization of small ovarian cancer deposits overexpressing Claudin-3/4 at the time of primary cytoreduction or at the time of interval surgical debulking for ovarian cancer. If CW800-c-CPE peptide is proven successful for the detection of ovarian cancer in patients, we believe it may have far-reaching effects for public health and the field of oncology because it may potentially be used to develop novel, highly sensitive real-time/diagnostic imaging modalities for other common cancers known to overexpress claudin-3/4 such as pancreatic, breast, and prostate cancer [44–47].

Supplementary Material

Refer to Web version on PubMed Central for supplementary material.

Acknowledgments

This work was supported in part by R01 CA154460-01 and U01 CA176067-01A1 grants from NIH, the Deborah Bunn Alley Foundation, the Tina Brozman Foundation, the Discovery to Cure Foundation, Ministero della Salute grant RF-2010-2313497, and the Guido Berlucchi Foundation to ADS. This investigation was also supported by NIH Research Grant CA-16359 from the NCI.

References

1. Siegel R, Ma J, Zou Z, Jemal A. Cancer statistics, 2014. CA: a cancer journal for clinicians. 2014; 64:9–29. [PubMed: 24399786]
2. Vitale SG, Marilli I, Lodato M, Tropea A, Cianci A. The role of cytoreductive surgery in advanced-stage ovarian cancer: a systematic review. Updates in surgery. 2013; 65:265–70. [PubMed: 23653397]
3. Coleman RL, Monk BJ, Sood AK, Herzog TJ. Latest research and treatment of advanced-stage epithelial ovarian cancer. Nature reviews Clinical oncology. 2013; 10:211–24.
4. van Dam GM, Themelis G, Crane LM, Harlaar NJ, Pleijhuis RG, Kelder W, Sarantopoulos A, de Jong JS, Arts HJ, van der Zee AG, Bart J, Low PS, et al. Intraoperative tumor-specific fluorescence imaging in ovarian cancer by folate receptor-alpha targeting: first in-human results. Nature medicine. 2011; 17:1315–9.

5. Chen YL, Chang MC, Huang CY, Chiang YC, Lin HW, Chen CA, Hsieh CY, Cheng WF. Serous ovarian carcinoma patients with high alpha-folate receptor had reducing survival and cytotoxic chemo-response. Molecular oncology. 2012; 6:360–9. [PubMed: 22265591]
6. Kennedy MD, Jallad KN, Thompson DH, Ben-Amotz D, Low PS. Optical imaging of metastatic tumors using a folate-targeted fluorescent probe. Journal of biomedical optics. 2003; 8:636–41. [PubMed: 14563201]
7. Crane LM, Arts HJ, van Oosten M, Low PS, van der Zee AG, van Dam GM, Bart J. The effect of chemotherapy on expression of folate receptor-alpha in ovarian cancer. Cellular oncology. 2012; 35:9–18.
8. Despierre E, Lambrechts S, Leunen K, Berteloot P, Neven P, Amant F, O'Shannessy DJ, Somers EB, Vergote I. Folate receptor alpha (FRA) expression remains unchanged in epithelial ovarian and endometrial cancer after chemotherapy. Gynecologic oncology. 2013; 130:192–9. [PubMed: 23558051]
9. Santin AD, Zhan F, Bellone S, Palmieri M, Cane S, Bignotti E, Anfossi S, Gokden M, Dunn D, Roman JJ, O'Brien TJ, Tian E, et al. Gene expression profiles in primary ovarian serous papillary tumors and normal ovarian epithelium: identification of candidate molecular markers for ovarian cancer diagnosis and therapy. International journal of cancer Journal international du cancer. 2004; 112:14–25. [PubMed: 15305371]
10. Bignotti E, Tassi RA, Calza S, Ravaggi A, Bandiera E, Rossi E, Donzelli C, Pasinetti B, Pecorelli S, Santin AD. Gene expression profile of ovarian serous papillary carcinomas: identification of metastasis-associated genes. American journal of obstetrics and gynecology. 2007; 196:245.e1–11. [PubMed: 17346539]
11. Bignotti E, Tassi RA, Calza S, Ravaggi A, Romani C, Rossi E, Falchetti M, Odicino FE, Pecorelli S, Santin AD. Differential gene expression profiles between tumor biopsies and short-term primary cultures of ovarian serous carcinomas: identification of novel molecular biomarkers for early diagnosis and therapy. Gynecologic oncology. 2006; 103:405–16. [PubMed: 16725184]
12. Bellone S, Tassi R, Betti M, English D, Cocco E, Gasparrini S, Bortolomai I, Black JD, Todeschini P, Romani C, Ravaggi A, Bignotti E, et al. Mammaglobin B (SCGB2A1) is a novel tumour antigen highly differentially expressed in all major histological types of ovarian cancer: implications for ovarian cancer immunotherapy. British journal of cancer. 2013; 109:462–71. [PubMed: 23807163]
13. Santin AD, Cane S, Bellone S, Palmieri M, Siegel ER, Thomas M, Roman JJ, Burnett A, Cannon MJ, Pecorelli S. Treatment of chemotherapy-resistant human ovarian cancer xenografts in C. B-17/SCID mice by intraperitoneal administration of Clostridium perfringens enterotoxin. Cancer research. 2005; 65:4334–42. [PubMed: 15899825]
14. Stewart JJ, White JT, Yan X, Collins S, Drescher CW, Urban ND, Hood L, Lin B. Proteins associated with Cisplatin resistance in ovarian cancer cells identified by quantitative proteomic technology and integrated with mRNA expression levels. Molecular & cellular proteomics: MCP. 2006; 5:433–43. [PubMed: 16319398]
15. Casagrande F, Cocco E, Bellone S, Richter CE, Bellone M, Todeschini P, Siegel E, Varughese J, Arin-Silasi D, Azodi M, Rutherford TJ, Pecorelli S, et al. Eradication of chemotherapy-resistant CD44+ human ovarian cancer stem cells in mice by intraperitoneal administration of Clostridium perfringens enterotoxin. Cancer. 2011; 117:5519–28. [PubMed: 21692061]
16. McClane BA. An overview of Clostridium perfringens enterotoxin. Toxicon: official journal of the International Society on Toxinology. 1996; 34:1335–43. [PubMed: 9027990]
17. Katahira J, Sugiyama H, Inoue N, Horiguchi Y, Matsuda M, Sugimoto N. Clostridium perfringens enterotoxin utilizes two structurally related membrane proteins as functional receptors in vivo. The Journal of biological chemistry. 1997; 272:26652–8. [PubMed: 9334247]
18. Katahira J, Inoue N, Horiguchi Y, Matsuda M, Sugimoto N. Molecular cloning and functional characterization of the receptor for Clostridium perfringens enterotoxin. The Journal of cell biology. 1997; 136:1239–47. [PubMed: 9087440]
19. English DP, Santin AD. Claudins Overexpression in Ovarian Cancer: Potential Targets for Clostridium Perfringens Enterotoxin (CPE) Based Diagnosis and Therapy. International journal of molecular sciences. 2013; 14:10412–37. [PubMed: 23685873]

20. Cocco E, Casagrande F, Bellone S, Richter CE, Bellone M, Todeschini P, Holmberg JC, Fu HH, Montagna MK, Mor G, Schwartz PE, Arin-Silasi D, et al. Clostridium perfringens enterotoxin carboxy-terminal fragment is a novel tumor-homing peptide for human ovarian cancer. BMC cancer. 2010; 10:349. [PubMed: 20598131]
21. Troyan SL, Kianzad V, Gibbs-Strauss SL, Gioux S, Matsui A, Oketokoun R, Ngo L, Khamene A, Azar F, Frangioni JV. The FLARE intraoperative near-infrared fluorescence imaging system: a first-inhuman clinical trial in breast cancer sentinel lymph node mapping. Annals of surgical oncology. 2009; 16:2943–52. [PubMed: 19582506]
22. Richter CE, Cocco E, Bellone S, Silasi DA, Ruttinger D, Azodi M, Schwartz PE, Rutherford TJ, Pecorelli S, Santin AD. High-grade, chemotherapy-resistant ovarian carcinomas overexpress epithelial cell adhesion molecule (EpCAM) and are highly sensitive to immunotherapy with MT201, a fully human monoclonal anti-EpCAM antibody. American journal of obstetrics and gynecology. 2010; 203:582.e1–7. [PubMed: 20870202]
23. Markman M. An update on the use of intraperitoneal chemotherapy in the management of ovarian cancer. Cancer journal. 2009; 15:105–9.
24. Huang R, Vider J, Kovar JL, Olive DM, Mellinghoff IK, Mayer-Kuckuk P, Kircher MF, Blasberg RG. Integrin alphavbeta3-targeted IRDye 800CW near-infrared imaging of glioblastoma. Clinical cancer research: an official journal of the American Association for Cancer Research. 2012; 18:5731–40. [PubMed: 22914772]
25. Santin AD, Zhan F, Cane S, Bellone S, Palmieri M, Thomas M, Burnett A, Roman JJ, Cannon MJ, Shaughnessy J Jr, Pecorelli S. Gene expression fingerprint of uterine serous papillary carcinoma: identification of novel molecular markers for uterine serous cancer diagnosis and therapy. British journal of cancer. 2005; 92:1561–73. [PubMed: 15785748]
26. Yoshida H, Sumi T, Zhi X, Yasui T, Honda K, Ishiko O. Claudin-4: a potential therapeutic target in chemotherapy-resistant ovarian cancer. Anticancer research. 2011; 31:1271–7. [PubMed: 21508375]
27. Marshall MV, Draney D, Sevick-Muraca EM, Olive DM. Single-dose intravenous toxicity study of IRDye 800CW in Sprague-Dawley rats. Molecular imaging and biology: MIB: the official publication of the Academy of Molecular Imaging. 2010; 12:583–94. [PubMed: 20376568]
28. Luo S, Zhang E, Su Y, Cheng T, Shi C. A review of NIR dyes in cancer targeting and imaging. Biomaterials. 2011; 32:7127–38. [PubMed: 21724249]
29. Ishizawa T, Fukushima N, Shibahara J, Masuda K, Tamura S, Aoki T, Hasegawa K, Beck Y, Fukayama M, Kokudo N. Real-time identification of liver cancers by using indocyanine green fluorescent imaging. Cancer. 2009; 115:2491–504. [PubMed: 19326450]
30. Vahrmeijer AL, Hutteman M, van der Vorst JR, van de Velde CJ, Frangioni JV. Image-guided cancer surgery using near-infrared fluorescence. Nature reviews Clinical oncology. 2013; 10:507–18.
31. Kitai T, Inomoto T, Miwa M, Shikayama T. Fluorescence navigation with indocyanine green for detecting sentinel lymph nodes in breast cancer. Breast cancer. 2005; 12:211–5. [PubMed: 16110291]
32. Unno N, Suzuki M, Yamamoto N, Inuzuka K, Sagara D, Nishiyama M, Tanaka H, Konno H. Indocyanine green fluorescence angiography for intraoperative assessment of blood flow: a feasibility study. European journal of vascular and endovascular surgery: the official journal of the European Society for Vascular Surgery. 2008; 35:205–7.
33. Tagaya N, Yamazaki R, Nakagawa A, Abe A, Hamada K, Kubota K, Oyama T. Intraoperative identification of sentinel lymph nodes by near-infrared fluorescence imaging in patients with breast cancer. American journal of surgery. 2008; 195:850–3. [PubMed: 18353274]
34. Ma Y, Tong S, Bao G, Gao C, Dai Z. Indocyanine green loaded SPIO nanoparticles with phospholipid-PEG coating for dual-modal imaging and photothermal therapy. Biomaterials. 2013; 34:7706–14. [PubMed: 23871538]
35. Chen W, Ayala-Orozco C, Biswal NC, Perez-Torres C, Bartels M, Bardhan R, Stinnet G, Liu XD, Ji B, Deorukhkar A, Brown LV, Guha S, et al. Targeting pancreatic cancer with magneto-fluorescent theranostic gold nanoshells. Nanomedicine. 2014; 9:1209–22. [PubMed: 24063415]

36. Tanaka E, Choi HS, Fujii H, Bawendi MG, Frangioni JV. Image-guided oncologic surgery using invisible light: completed pre-clinical development for sentinel lymph node mapping. Annals of surgical oncology. 2006; 13:1671–81. [PubMed: 17009138]
37. Sampath L, Kwon S, Ke S, Wang W, Schiff R, Mawad ME, Sevick-Muraca EM. Dual-labeled trastuzumab-based imaging agent for the detection of human epidermal growth factor receptor 2 overexpression in breast cancer. Journal of nuclear medicine: official publication, Society of Nuclear Medicine. 2007; 48:1501–10.
38. Keereweer S, Mol IM, Vahrmeijer AL, Van Driel PB, Baatenburg de Jong RJ, Kerrebijn JD, Lowik CW. Dual wavelength tumor targeting for detection of hypopharyngeal cancer using near-infrared optical imaging in an animal model. International journal of cancer Journal international du cancer. 2012; 131:1633–40. [PubMed: 22234729]
39. Terwisscha van Scheltinga AG, van Dam GM, Nagengast WB, Ntziachristos V, Hollema H, Herek JL, Schroder CP, Kosterink JG, Lub-de Hoog MN, de Vries EG. Intraoperative near-infrared fluorescence tumor imaging with vascular endothelial growth factor and human epidermal growth factor receptor 2 targeting antibodies. Journal of nuclear medicine: official publication, Society of Nuclear Medicine. 2011; 52:1778–85.
40. Hidalgo M, Amant F, Biankin AV, Budinska E, Byrne AT, Caldas C, Clarke RB, de Jong S, Jonkers J, Maelandsmo GM, Roman-Roman S, Seoane J, et al. Patient-derived xenograft models: an emerging platform for translational cancer research. Cancer discovery. 2014; 4:998–1013. [PubMed: 25185190]
41. Furukawa N, Oi H, Yoshida S, Shigetomi H, Kanayama S, Kobayashi H. The usefulness of photodynamic eye for sentinel lymph node identification in patients with cervical cancer. Tumori. 2010; 96:936–40. [PubMed: 21388055]
42. Wapnir I, Dua M, Kieryn A, Paro J, Morrison D, Kahn D, Meyer S, Gurtner G. Intraoperative imaging of nipple perfusion patterns and ischemic complications in nipple-sparing mastectomies. Annals of surgical oncology. 2014; 21:100–6. [PubMed: 24046104]
43. Marano A, Priora F, Lenti LM, Ravazzoni F, Quarati R, Spinoglio G. Application of fluorescence in robotic general surgery: review of the literature and state of the art. World journal of surgery. 2013; 37:2800–11. [PubMed: 23645129]
44. Michl P, Buchholz M, Rolke M, Kunsch S, Lohr M, McClane B, Tsukita S, Leder G, Adler G, Gress TM. Claudin-4: a new target for pancreatic cancer treatment using Clostridium perfringens enterotoxin. Gastroenterology. 2001; 121:678–84. [PubMed: 11522752]
45. Kominsky SL, Tyler B, Sosnowski J, Brady K, Doucet M, Nell D, Smedley JG 3rd, McClane B, Brem H, Sukumar S. Clostridium perfringens enterotoxin as a novel-targeted therapeutic for brain metastasis. Cancer research. 2007; 67:7977–82. [PubMed: 17804705]
46. Long H, Crean CD, Lee WH, Cummings OW, Gabig TG. Expression of Clostridium perfringens enterotoxin receptors claudin-3 and claudin-4 in prostate cancer epithelium. Cancer research. 2001; 61:7878–81. [PubMed: 11691807]
47. Facchetti F, Lonardi S, Gentili F, Bercich L, Falchetti M, Tardanico R, Baronchelli C, Lucini L, Santin A, Murer B. Claudin 4 identifies a wide spectrum of epithelial neoplasms and represents a very useful marker for carcinoma versus mesothelioma diagnosis in pleural and peritoneal biopsies and effusions. Virchows Archiv: an international journal of pathology. 2007; 451:669–80. [PubMed: 17609977]

Novelty and Impact

The amount of residual disease is a crucial prognostic factor during the primary surgery for ovarian cancer.

We show that the carboxy-terminal fragment of *Clostridium Perfringens Enterotoxin* (c-CPE), conjugated to fluorescent fluorophores, is able to specifically identify microscopic tumor deposits in pre-clinical models of chemotherapy naïve and chemotherapy-resistant ovarian cancer following IP or IV injection. Fluorescent c-CPE may provide a novel tumor-specific tool that can assist the surgeon to identify residual disease at the time of debulking surgery.

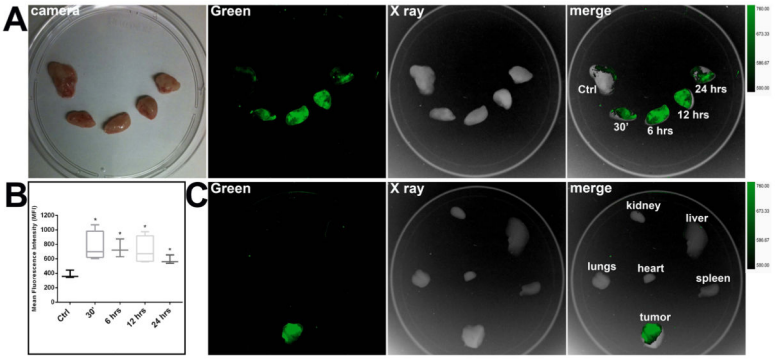

Figure 1.

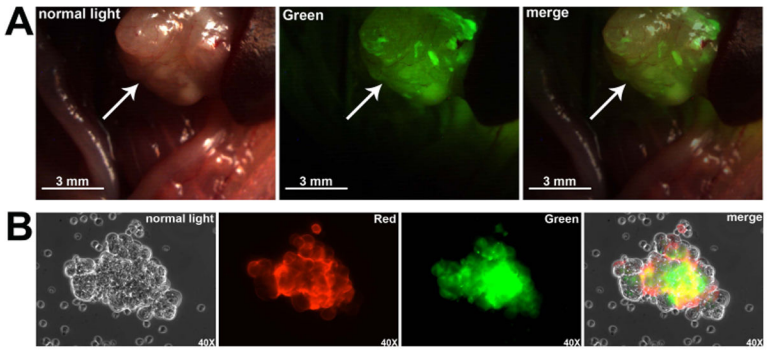

Figure 2.

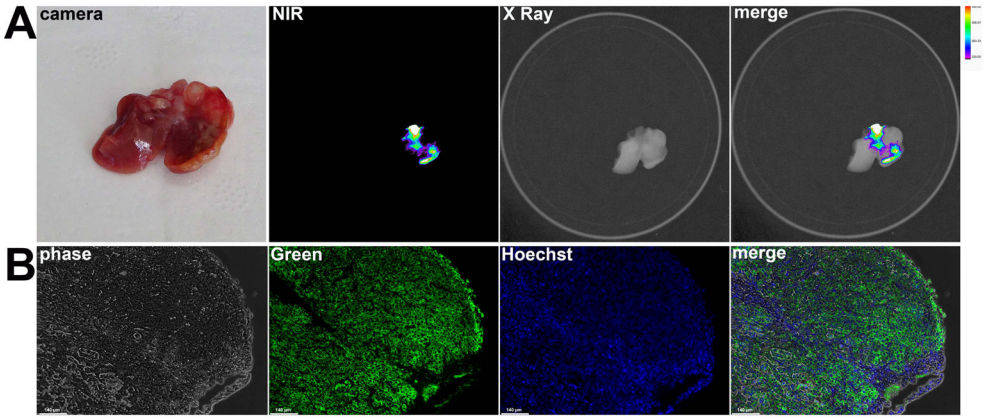

Figure 3.

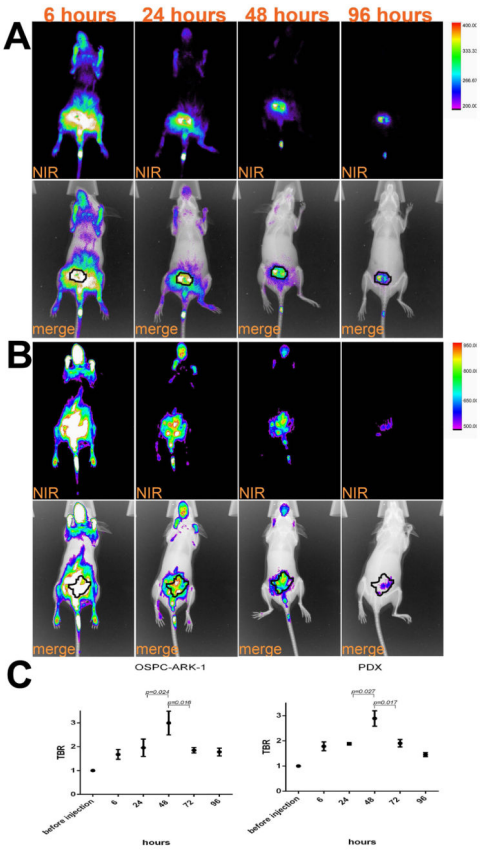

Figure 4.

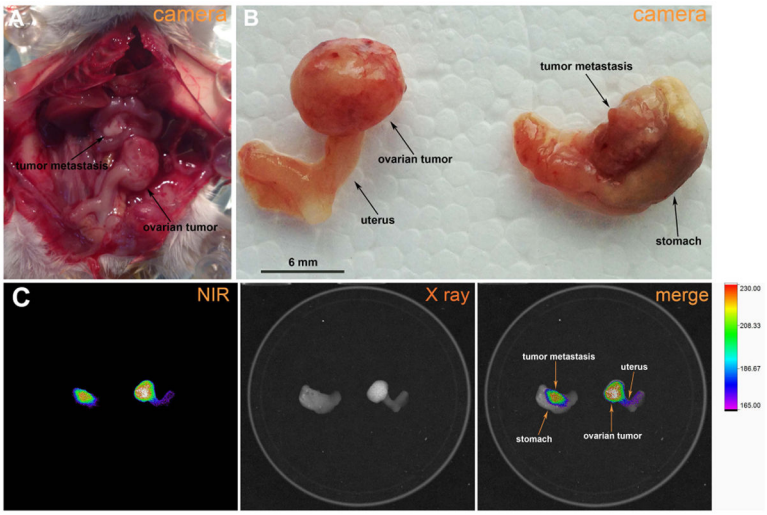

Figure 5.

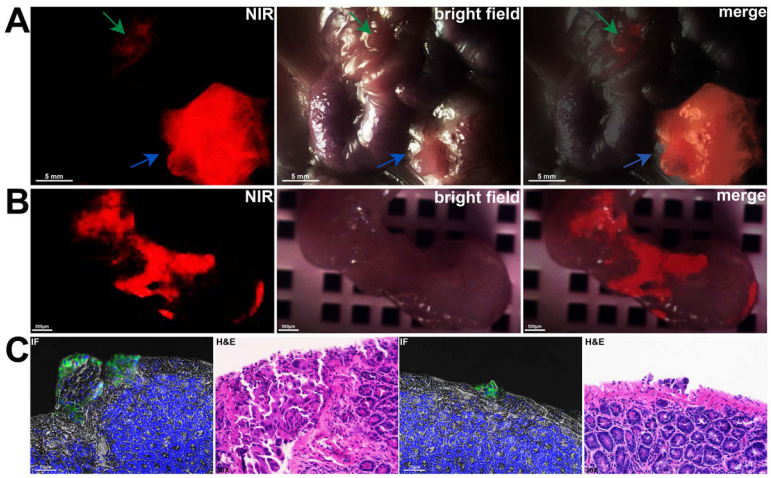

Figure 6.